Am J Transl Res 2018;10(11):3555-3566
www.ajtr.org /ISSN:1943-8141/AJTR0053979

Original Article

Gene expression profiling: identification of gene expression in human MSC chondrogenic differentiation

Ming Gong[1,3*], Tangzhao Liang[2*], Hao Zhang[1*], Shaochu Chen[1], Yawei Hu[1], Jianhua Zhou[1], Xuan Zhang[1], Wang Zhang[1], Xiaojing Geng[4], Xuenong Zou[3]

[1]Department of Spinal Surgery, People's Hospital of Longhua, Shenzhen 518109, P. R. China; [2]Department of Orthopedic Surgery, The Third Affiliated Hospital of Sun Yat-sen University, Guangzhou 510080, P. R. China; [3]Guangdong Provincial Key Laboratory of Orthopaedics and Traumatology, Orthopaedic Research Institute/Department of Spinal Surgery, The First Affiliated Hospital of Sun Yat-sen University, Guangzhou 510080, P. R. China; [4]Department of Aging Medicine, The Fifth Affiliated Hospital of Sun Yat-sen University, Zhuhai 519000, P. R. China. [*]Equal contributors.

Received March 28, 2017; Accepted September 5, 2018; Epub November 15, 2018; Published November 30, 2018

Abstract: Understanding the mechanisms that govern cell fate will lead to the development of techniques for the induction of human mesenchymal stem cell differentiation into desired cell outcomes and the production of an autologous source of tissue for regenerative medicine. Here, we demonstrate that stem cells derived from adult bone marrow grown with 3D pellets take on characteristics similar to human cartilage. The NFAT signaling pathway is primarily linked to cell differentiation and influences chondrogenic differentiation. Based on our previous results that alterations in the expression of the NFATc1 gene affect chondrogenesis, we screened a microarray and identified 29 genes with altered expression, including 13 up-regulated (fold change ≥ 2) and 16 down-regulated (fold change ≤ 2) genes, compared with the control group. We then used RT-PCR to validate the chip data. Gene ontology and pathway analyses were performed on these altered genes. We found that these altered genes function in the complement and coagulation cascades, metabolism, biosynthesis, transcriptional regulation, proteolysis, and intracellular signaling pathways, such as the cytoplasmic calcineurin-dependent signaling pathway, the cyclin-dependent kinase inhibitor 2C signaling pathway, the MAPK signaling pathway, and the insulin signaling pathway. Our study suggests that these pathways may play important roles in chondrogenesis, which could be useful in the design of biomaterials.

Keywords: Human mesenchymal stem cells (hMSCs), gene microarray, nuclear factor of activated T-cells (NFAT)

Introduction

Due to its avascular nature, cartilage tissue has been regarded as having limited regenerative capacity following injury. Human mesenchymal stem cells (hMSCs) are multipotential cells that can be derived from patient cells obtained during an operation and may provide an autologous source of tissue for regenerative medicine. As they have been induced to differentiate into myocytes, adipocytes, osteoblasts and chondrocytes in response to specific culture conditions and treatments [1, 2], hMSCs may serve as a useful and convenient system for studying the effects and mechanism of chondrogenesis.

It has been shown that chondrogenesis and osteogenesis *in vivo* could not only produce bone-matrix compositions, acid mucopolysaccharide and collagen but also provide the calcium salt for crystal deposition. Calcium [Ca^{2+}] signaling cascades have been linked to vertebrate development and the growth and differentiation of multiple cell types [3, 4]. Additionally, calcineurin activity has been shown to enhance the functionality of nuclear factor of activated T-cells (NFAT). [Ca^{2+}] acts as a switch for NFAT activity by regulating its phosphorylation status. In resting cells, phosphorylated NFAT is retained in the cytoplasm, while dephosphorylated NFAT (mediated by [Ca^{2+}]) translocates to the nucleus and binds to its target promoter regions [5, 6]. Previous research indicated that the calcineurin/NFAT pathway is primarily linked to cell differentiation and influences chondrogenic differentiation [3, 5]. NFAT4 and NFATc1 both induce cartilage gene expres-

Table 1. Patient characteristics

Characteristics	
Patients (n)	24
Median age	44
Female/male	10/14
Source of cell (bone marrow)	Spine internal fixation

sion [7]. Interestingly, recent studies have suggested that Sox9 contains an NFAT binding element in its promoter region [8]. In contrast, NFAT1/NFATc2 is generally regarded as an inhibitor of chondrogenesis based primarily on neoplastic cartilage proliferation in and around the articular cartilage of adult $Nfat^{-/-}$ mouse appendicular joints [9, 10].

In our previous study, we found that NFATc1 expression increases in the murine cell line C3H10T1/2 and that the NFATc1 protein is able to bind to the promoter region of Sox9, which is a master transcription factor in initiating chondrogenic differentiation. In this study, we sought to determine whether NFATc1 gene expression was also upregulated in chondrogenic differentiation of hMSCs and whether this upregulation could regulate a similar differentiation pathway. Moreover, to elucidate possible signaling pathways involved in differentiation and NFATc1 signaling, we performed this study on pellet samples from 24 patients using Agilent one-color cDNA arrays. Then, we applied microarray technology to screen out both subtypes of potential genes and regulated pathways. The changes in global gene expression that occurred in response to the differentiation following 3 days of in vitro culture were determined and further analyzed with bioinformatics tools.

The goal of this study was to identify candidate genes associated with the chondrogenesis of hMSCs and to provide novel insights into the transcriptionally regulated pathways involved in the differentiation. We found that NFATc1 mRNA was highly expressed, which was consistent with the results of our previous study. In addition, we identified the major clusters of upregulated and downregulated genes, which were subjected to detailed analysis.

Material and methods

Patient characteristics and ethics statement

Human bone marrow (hBM) was collected from the drill holes of the pedicle during the internal spine fixation operations of 24 patients (14 men and 10 women, with a mean age of 44 years, SD age of 10 years) with degenerative and traumatic lumbar spondylolisthesis (**Table 1**). Written informed consent was obtained from patients undergoing hBM collection, and the sample of human articular cartilage was collected in a clinic case of excision of a bone tumor and artificial joint replacement. All the procedures were performed in accordance with the guidance and approval of the Institutional Review Boards in the First Affiliated Hospital of Sun Yat-sen University.

Isolation and cultivation of hMSCs and 3D pellet formation

hMSC isolation, cultivation, and identification using flow cytometry analysis, including multidifferentiation potential analysis to detect osteogenic, chondrogenic and adipogenic differentiation, were carried out following the procedures described in our previous studies. To induce chondrogenesis, 2.5×10^5 cells were grown first as a monolayer, collected using trypsin, and then pelleted by centrifugation at 1,200 rpm for 5 min (15 mL conical polypropylene tubes). The pellet was then cultured in 2 mL of chondrogenic medium (high glucose DMEM containing 2% FBS, 100 nM dexamethasone [Sigma, Dorset, UK], 50 mM L-ascorbic acid-2 phosphate [Sigma, Dorset, UK], BD™ ITS + Premix 1:100 [6.25 μg/mL insulin, 6.25 μg/mL transferrin, 6.25 ng/mL selenous acid, 1.25 mg/mL bovine serum albumin, and 5.35 mg/mL linoleic acid; BD Biosciences Discovery Labware, Bedford, MA, USA] and 10 ng/mL transforming growth factor-β_3 [TGF-β_3; PeproTech EC, London, UK].

Histology and immunohistochemistry and western blot

Human MSCs pellets that had been maintained for 21 days were fixed in 4% phosphate-buffered formalin for 10 min, processed into paraffin wax, sectioned into 5 μm sections, and stained with toluidine blue (1% toluidine blue) to detect sulfated proteoglycan (GAG) matrix deposition. The sections were washed three times with water and then with 95-100% ethanol. Images were captured using a Leica DMI-4000B microscope (Germany) fitted with an Optixcam summit series 5MP digital camera. The photographs were assembled in Adobe Photoshop 6.0.

Table 2. Nucleotide sequences of the RT-PCR primers

Gene	Product length (bp)	Primer sequence	
		Forward primer	Reverse primer
DNMT3A	92	5'GTCCAGGAACCTACCCATAA3'	5'GGGCAGCTACTTCCAGAG3'
PLCG2	61	5'GCCGAAGCAGAAGTAGCG3'	5'CGACTCGGGTCACTCAGC3'
ANXA11	68	5'GGCTCGGGACCCTCACTCA3'	5'CCGCCCACGTCCCATTT3'
CYTH2	108	5'CGTTCGGCTCAGTCGTAGA3'	5'CAGGCTCAGCCCAAACAAT3'
GRK6	61	5'GGCCCTGCGCCTTACA3'	5'GGAGGAGGAAGACGACGG3'
HSP90B1	76	5'TGGGTTCATGTTTCCCGTC3'	5'CCCACTACACCGCAAGCAG3'
KEAP1	84	5'CATCTCCCGATTTCGTTGC3'	5'GGCGCTGTGCGTTGTTA3'
NDST2	168	5'GCTGTTTGGAGGCTGTTTATG3'	5'GAAGGCTGAGGCAGGAGAAT3'
NSMAF	81	5'GACCTGCACTGCCGGATAGC3'	5'CGGGGACAGGAACTGGATGAC3'
TSPAN14	102	5'AGCTTCTCCGCGTTAGTCGT3'	5'CACAGTCCGCAGCCACAA3'
VCP	278	5'ACCCATACACCCATCTTCTCC3'	5'CTGTGGTTGCCCTTTGACTT3'
DUSP3	87	5'CTGGCTCGGGAGGCTGTA3'	5'GCCATGTCGGGCTCGTT3'
GTPBP5	83	5'CTCCTGCTTCCGCTACCA3'	5'CCCAAGGCTTGCCCAGT3'
INSIG1	98	5'GGGCCTTCCTCGCTCTT3'	5'GTGCAATCTGGGCATCG3'
OSMR	121	5'GGGACTGAAGGGAGGGAA3'	5'GGGCGGGAGTTACTGGAA3'
PPP1CA	198	5'CCCTGGGTGGAAGGTGTT3'	5'AGCCGTAGCTGTCTTTGAGTG3'
SH3RF1	72	5'CCTCCCTCATCTCCGCCT3'	5'AAAACTTCCCGCAGTCGTGT3'
SLC23A2	131	5'GAGCGCTGGTCCCTGAG3'	5'TAAAACATCCAACCCACTGAG3'
DYNC1I1	76	5'GGGAAAGGATGCTGTTTGATT3'	5'TCCGACTTGCAGGGTAGTG3'
SPTBN1	84	5'CCCTTCAGCTCCTGCCAC3'	5'GCCAGCCCACCTACCCA3'
BNC2	87	5'AAGAGGAAGGAGGGTGGAA3'	5'GGCCGCTAAGAGGAGAC3'
ENPP1	134	5'GTCCGGGAGTGCTTCTTCG3'	5'TGCTTTCACAGGCATCCATAA3'
FBXO42	76	5'CCGCCATCTTCCTCCACTC3'	5'GCTCTGCGCTGTCTTCTCC3'
JMY	119	5'CGAGTCGGACTGGGTGGCT3'	5'GGTTGTGGCAGGTTATGGCA3'
NFATC1	71	5'GGACCCGAACTCGCCTT3'	5'CCCGCCGGTCCTTCTA3'
PLCE1	140	5'AGGAGCCAAGAGGTGAGG3'	5'GACACTTTTCCGCCAGGT3'
RAB22A	136	5'GTGCCTGGCTTGAGGTTC3'	5'CCCTGTACTTTGTGGACTTGC3'
TCFL5	125	5'ACAGCGGCAGGAATGAAGAC3'	5'ACAGGCATGAGCCACAGAAC3'
ATOH8	74	5'AAGAAGCTCAAGCGGAAAG3'	5'TCCAAGTCCAGTCGGAAAGT3'
CDKN2C	81	5'GAGACTTGACGGGAGGAGGT3'	5'TCGCAGTCTCGCACGCT3'
KDSR	63	5'ACAGGAGGCCACTCACCA3'	5'CGCTCATCAGCCCCAAG3'
MALT1	113	5'CTCAGGAAGCCCAGACGC3'	5'CCTCCCGAGCAGGAAAG3'
NET1	140	5'CCGCTGGAAGTGAGGGTG3'	5'CAGTCAGGAGGCGAGGAGA3'
PTTG1IP	87	5'AGCTCCTTTCTCGGGTCC3'	5'GGAAGTTCATCTACAAGGGTCAT3'

Primer sequences and product size of genes that were further tested with real-time PCR.

Lysates were generated from the pellets that had been maintained for 3 days using RIPA buffer (50 mM Tris-HCl, pH 7.5; 150 mM NaCl; 1% NP-40; 0.25% sodium deoxycholate, and 1 mM EDTA) supplemented with a protease inhibitor cocktail (Sigma-Aldrich). The total protein concentration was determined using the Coomassie Bradford protein assay kit (Bio-Rad). After protein quantification, 1 μL of β-mercaptoethanol and bromphenol blue was added to each sample. Twenty (20) micrograms of each lysate was separated by electrophoresis on an 8% sodium dodecyl sulfate-polyacrylamide gel (SDS-PAGE) and then transferred onto a 0.45 μm PVDF membrane (Immobilon™, Millipore Corp., Bedford, MA). The membranes were blocked using a buffer containing TBS, 0.25% Tween-20, 0.1% serum from the species that the secondary antibody was raised in, and 5% nonfat milk for 1 h at room temperature. The membranes were probed overnight with mouse monoclonal anti-NFATc1 (1:200, Abcam) or rab-

bit polyclonal β-actin (1:2000, Abcam). They were then incubated with horseradish peroxidase-conjugated secondary antibodies (Jackson Immuno Research). The protein bands were visualized using the Super-Signal chemiluminescent detection module (Pierce) and exposed to x-ray film.

Total RNA extraction and reverse transcription quantitative PCR analysis

Total RNA was extracted from the hMSC pellets that had been maintained for 3 days or 3 weeks using TRIzol (Invitrogen, CA, USA), according to the manufacturer's instructions. cDNA was synthesized from 0.5 μg of total RNA with an oligo-dT primer using a commercially available kit according to the manufacturer's protocol (TaKaRa, Japan). The oligonucleotide primers used to amplify the target mRNA are listed in **Table 2**. The mRNA expression level of each target gene was normalized to GAPDH expression from the same sample. The PCR reaction conditions were as follows: an initial denaturation step at 95°C for 10 mins, followed by 40 cycles of 95°C for 10 s and 60°C for 30 s. Each experiment was performed in a real-time PCR system (CFX Connect™ Real-time system, BIO-RAD, USA). The expression levels of mRNAs were detected using an RT kit (TaKaRa, Japan). The relative expression levels of all the genes were calculated using the $2^{-\Delta\Delta Ct}$ method.

Bioinformatics analysis

Microarray hybridization: Cyanine-3 (Cy3) labeled cRNA was prepared from 0.5 μg of eligible RNA using the One-Color Low RNA Input Linear Amplification PLUS kit (Agilent Technologies, USA) according to the manufacturer's instructions (Kang Chen Bio-tech, Shanghai, China) for microarray hybridization. Dye incorporation and cRNA yield were checked with the NanoDrop-1000 Spectrophotometer. Then, 1.5 μg of cRNA with the incorporation of > 10 pmol Cy3/μg cRNA was hybridized to the Whole Human Genome Oligo Microarray (4x44K, Agilent Technologies) according to the manufacturer's instructions. The human whole-genome microarray covered more than 27,958 unique human genes and transcripts. The processed slides were scanned and the resulting text files were extracted with Feature Extraction Software version 10.7.3.1 (Agilent Technologies, USA). Quantile normalization and subsequent data processing were performed using the GeneSpring GX v11.5.1 software package (Agilent Technologies). After quantile normalization of the raw data, genes that had flags in at least 3 out of 6 groups in Detected ("All Targets Value") were chosen for further data analysis. Differentially expressed genes were identified through fold-change screening.

Hierarchical clustering and series tests of cluster (STC)

To ascertain whether differentially expressed genes among groups were selected correctly, unsupervised hierarchical cluster analysis was done for the human genes and transcripts represented. Spearman correlation was used as a similarity measure between samples. Next, gene expression profiles were analyzed using a method called "Series tests of cluster" (STC), which extracts significant patterns by calculating the correlations of gene expression and then identifying significant genes based on their correlations with a specific pattern. Each extracted pattern represented a set of coexpressed genes for further study.

Gene ontology (GO) category and pathway analyses

Differently expressed genes were grouped on the basis of the Gene Ontology (GO) consortium (*http://www.geneontology.org/*). GO analysis was applied in order to organize genes into hierarchical categories and uncover the coexpression network on the basis of biological process and molecular function. Meanwhile, pathway analyses were performed based on the basis of scoring by KEGG (*http://www.genome.jp/kegg/*) and Biocarta (*http://www.biocarta.com/*). Fisher's exact test and the chi-square test were used to classify the enrichment of both GO and pathway category. The *P*-value cutoff, which denotes the significance of GO item and pathway, was 0.05. Unsupervised hierarchical clustering was performed using Agilent GeneSpring GX software. GO analysis and pathway analyses were performed in the standard enrichment computation method.

Data analysis and statistical analysis

In RT-PCR testing, each experiment was repeated at least three times. Data are presented as the mean ± S.D. Comparisons between groups

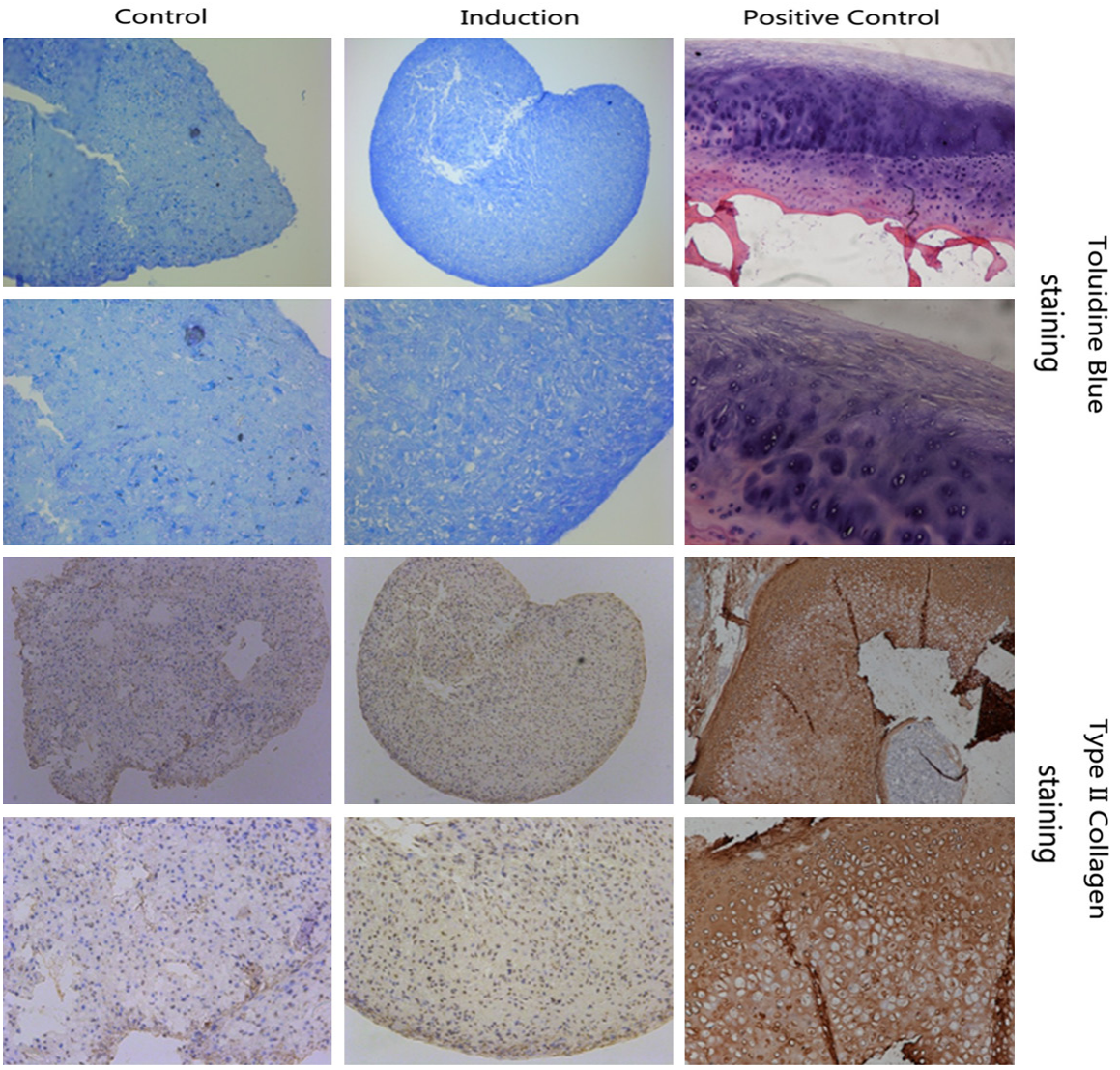

Figure 1. Serial paraffin sections of pellet after 21 days were stained with toluidine blue; representative images are shown. Scale bar = 100 um.

were performed using the Mann-Whitney test unless otherwise indicated. Statistical significance was determined using a two-tailed distribution assumption. Statistically significant results are denoted using *P < 0.05.

Results

Histochemistry staining for hMSC pellets

We first assessed the deposition of extracellular matrix (ECM) in the pellets by toluidine blue staining at 21 days, which was used to determine the phases of chondrocyte hypertrophy. The induced pellets appeared similar to human articular cartilage, which we used as a positive control (**Figure 1**). Compared with the surrounding area of the positive group, the induced pellets had a greater proportion of surrounding ECM, which was condensed in a stripe, while the cell nucleus was intensely stained. In addition, for collagen II staining, we also found positive staining located in the same area in the induced samples. In the control group, the pellet tissue was so soft that it could not sustain a spherical shape. The positive staining was significantly observed in the induced group but not in the control pellets.

Chondrogenic marker gene expression

We detected gene expression consistent with chondrogenesis in the pellet model. The pellet

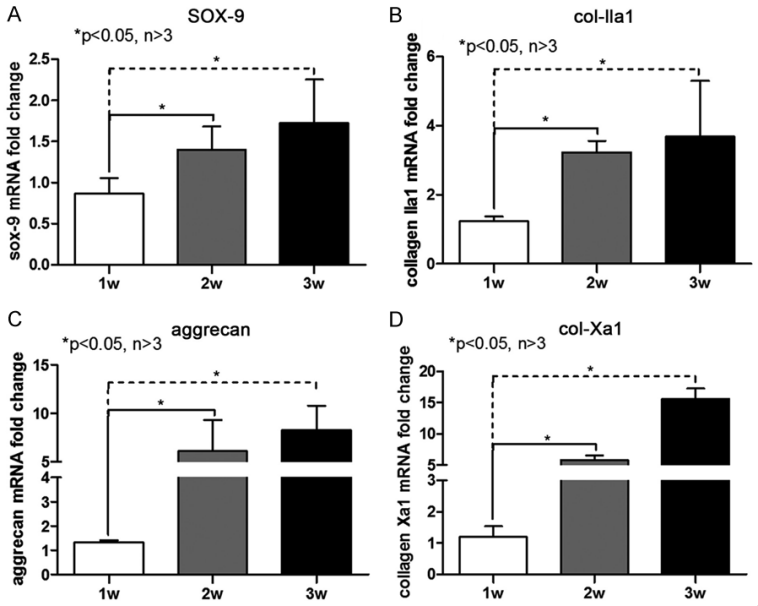

Figure 2. Real-time quantitative RT-PCR analysis of Sox-9, Col2A1, aggrecan, Col10A1 mRNA expressions in the induced-cartilage tissues from pellet cultures at day 21. COL1A1 type I collagen a-chain; COL2A1 type II collagen a-chain; COL10A1 type X collagen a-chain. Relative expression levels of each gene were obtained by using the $2^{-\Delta\Delta Ct}$ method. The bars represent means ± SD (n = 3: *P < 0.05).

samples were collected following 7, 14, and 21 days of differentiation and assayed for gene expression of Sox-9, collagen IIa1, aggrecan, and collagen Xa1 by RT-PCR. At the end of 7 days, the expression of Sox-9 (**Figure 2A**), collagen IIa1 (**Figure 2B**), aggrecan (**Figure 2C**), and collagen Xa1 (**Figure 2D**) showed no significant changes compared with the control (normalized as 1). However, they were all upregulated at days 14 and 21. The expression of all genes increased from day 7 to day 21, and the expression was significantly higher at end of differentiation. Our results suggested that this pellet model was able to differentiate into cartilage.

Profiling of gene expression in hMSC chondrogenic differentiation

As our previous study showed, transcriptional changes are likely to initiate in the early stage of day 3. We used Agilent one color human microarrays (4x44K, Agilent Technologies, USA) to monitor gene expression at day 3 and elucidate the possible mechanisms of the differentiation. The microarray probe represented 27,958 unique human genes and transcripts. Genes were set as significant if they were differentially expressed above a threshold (Fold Change ≥ 1.5, *P* value ≤ 0.05) in this experiment. As shown in **Figure 3**, the comparison analysis revealed 426 upregulated genes and 338 downregulated genes (**Figure 3A**). Unsupervised hierarchical clustering (**Figure 3B**) showed a distinguishable gene expression profile among the control and induction groups.

Bioinformatics analysis

To systematically identify biological connections of differentially expressed genes and identify new pathways associated with chondrogenesis of hMSCs, we performed KEGG pathway and GO analysis. Upregulation was particularly noted for genes involved in metabolic processes, as 4 of the top 10 terms were significantly downregulated in biological processes (BP) (**Figure 5A**). The remaining 6 genes that were upregulated were concentrated in osteoclast differentiation pathways (**Figure 4A**). Consistent with the GO results, pathway analysis also showed a downregulation of metabolic regulators, particularly those responsible for the regulation of BP and skeletal system development (**Table 3**). This was exemplified by the reduction of the phospholipase C, gamma 2 (PLCG2), and phosphatidylinositol-specific gene families. In addition, mineral absorption was also downregulated, as evidenced by the reduction of SLC-23A2 (solute carrier family 23, member 2) and glycosaminoglycan synthesis, such as N-deacetylase/N-sulfotransferase 2 (NDST2). In GO graphs where an annotated gene moves from a more general to more specific function, the genes involved in the biological regulation of osteoclast differentiation (**Figure 5A**) and skeletal system development were downregulated in KEGG analysis (**Figure 5B**). In the case of downregulated BP (**Figure 4B**), the nuclear factor of activated T-cells (cytoplasmic, calcineurin-dependent process) played a crucial part in the differentiation, which is consistent with the important role of inflammation in the initiation and early stage of chondrogenesis.

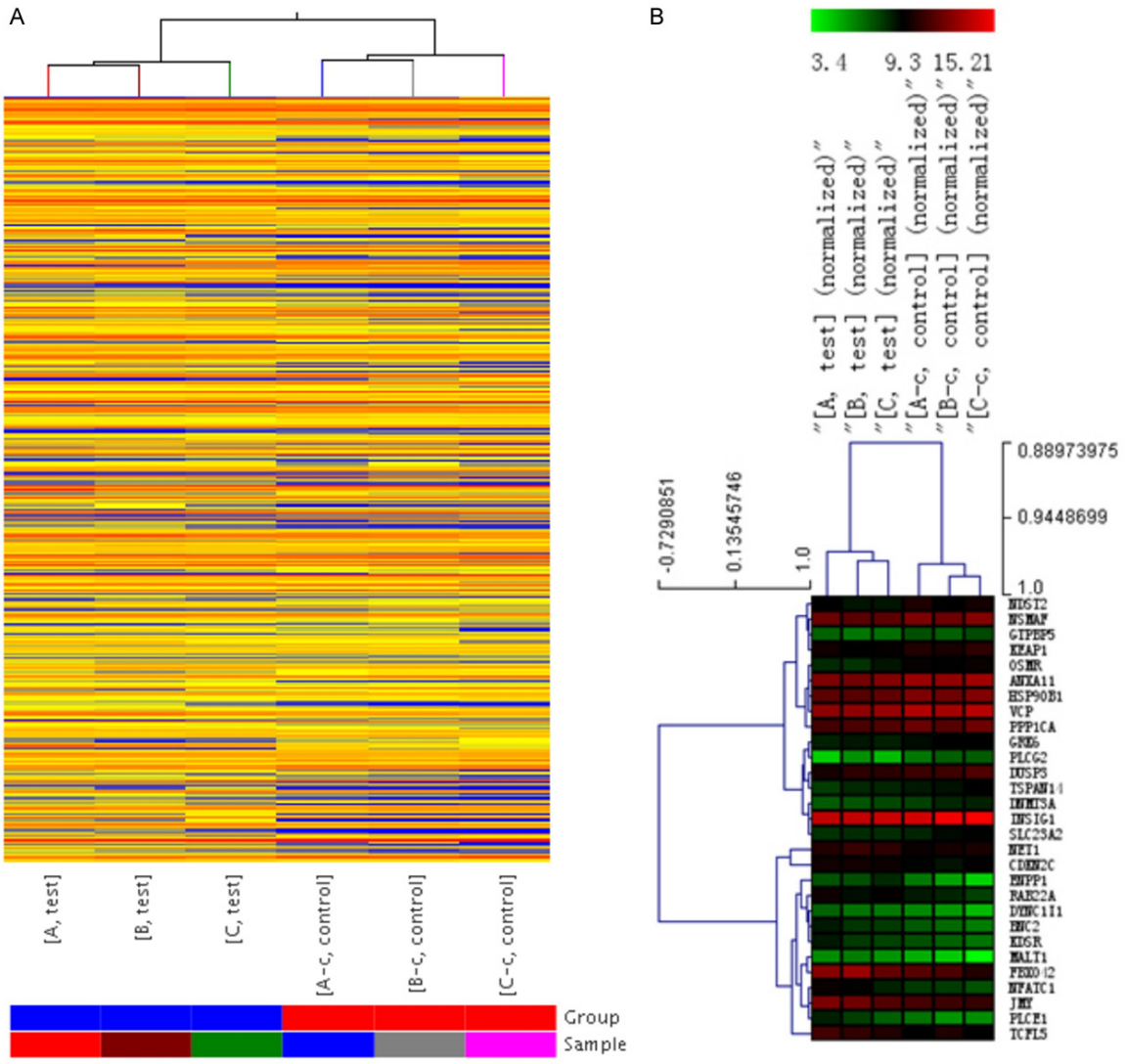

Figure 3. Hierarchical Clustering on "Differentially expressed genes in test vs control". "Red" indicates high relative expression, and "blue" indicates low relative expression.

Validation of microarray results by RT-PCR and protein assay

The up- and downregulated mRNAs are shown in **Tables 4** and **5** and represent the most striking altered transcripts of chondrogenesis. To confirm the chip results, 13 upregulated genes were verified by qRT-PCR (**Figure 6A**). The expression of DYNC1I1, BNC2, ENPP1, FBXO42, JMY, NFATC1, PLCE1, RAB22A, TCFL5, ATOH8, CDKN2C, KDSR, MALT1 and NET1 was markedly increased, and the expression of DNMT3A, PLCG2, ANXA11, GRK6, HSP90B1, KEAP1, NDST2, NSMAF, TSPAN14, VCP, DUSP3, GTPBP5, INSIG1, OSMR, PPP1CA and SLC23A2 was dramatically repressed (**Figure 6B**). The results showed BNC2, ENPP1, FBXO42 and NFATc1 expression patterns similar to those observed in the microarray experiments, among which PLCG2 and SLC23A2 mRNA expression was confirmed to be downregulated significantly (Fold change > 2). Western blot analysis showed that the level of NFATc1 protein was increased in hMSC pellet chondrogenesis (**Figure 6B**). These results were consistent with microarray data.

Discussion

High-density cell culture is pivotal for the chondrogenic differentiation of human mesenchymal stem cells (hMSCs). This system provides a

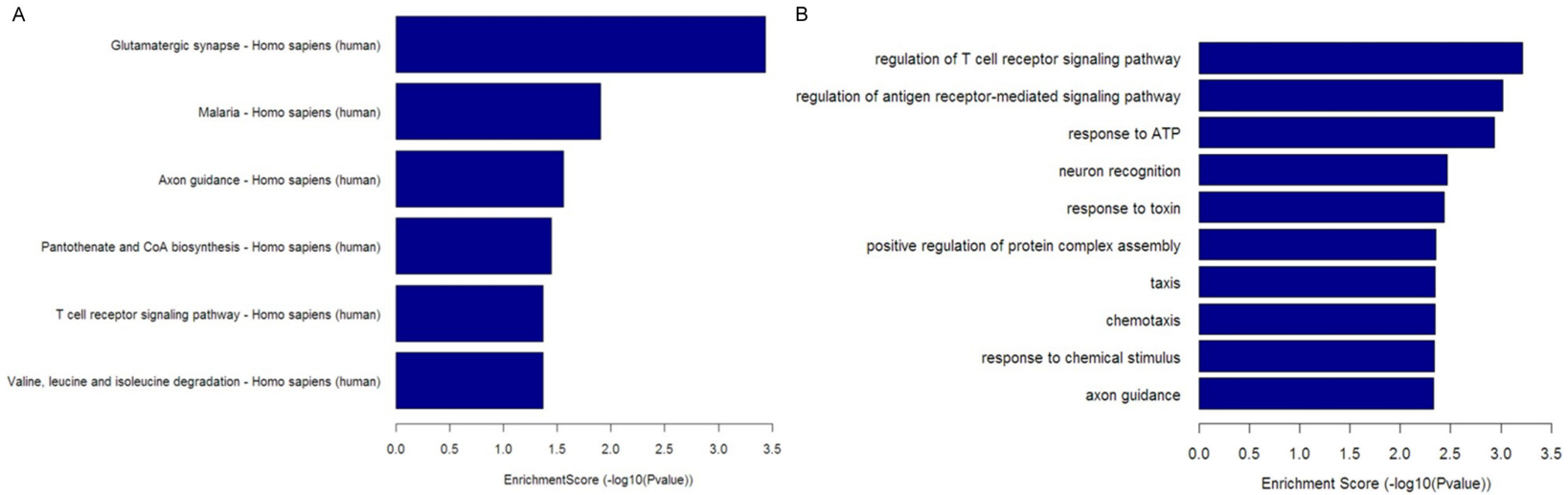

Figure 4. A: Top 6 up-regulated biological process terms based on Gene Ontology (GO) analysis. B: Top 10 up-regulated pathways based on KEGG and Biocarta databases. Enrichment score equals -Lg *P* value, where P represents the significance testing value.

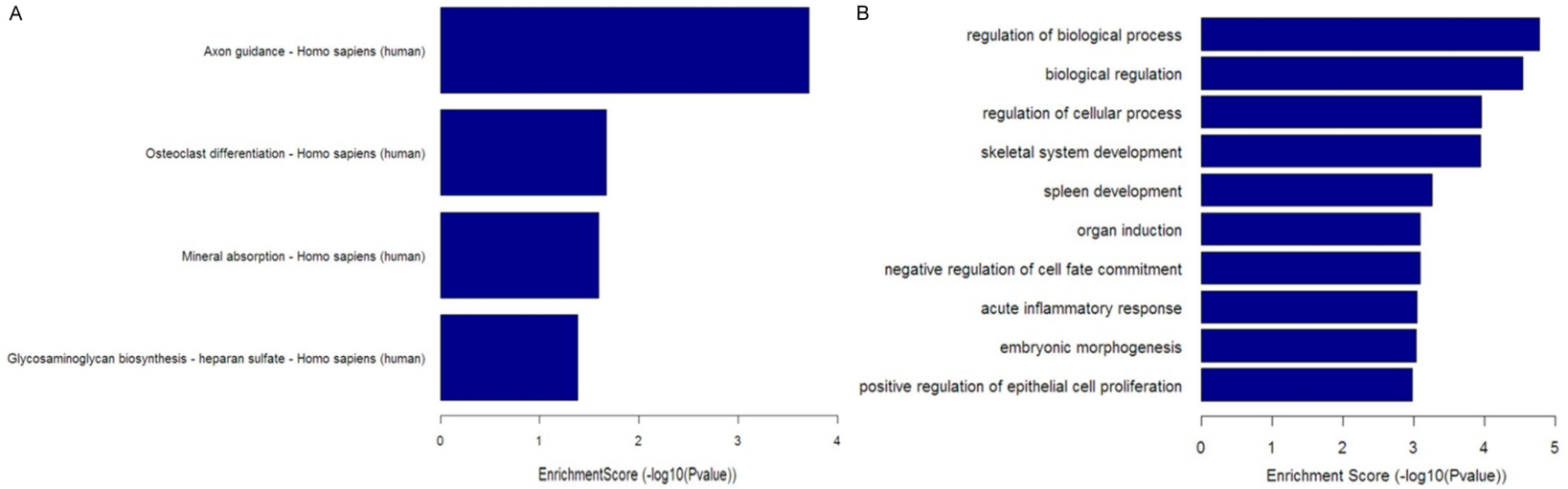

Figure 5. A: Top 4 down-regulated biological process terms based on Gene Ontology (GO) analysis. B: Top 10 down-regulated pathways based on KEGG and Biocarta databases. Enrichment score equals -Lg *P* value, where P represents the significance testing value.

Table 3. Pathway analysis by KEGG database up and down

Pathway (Homo sapiens)	Gene symbol	*p*-value	Enrichment
Up-regulated			
Glutamatergic synapse	ADRBK2//GLS//GNAI3//GRIK2//GRIN2D//GRIN3B//HOMER2//SLC1A1//SLC1A2	0.02869261	3.434325
Malaria	COMP//IL18//PECAM1//SDC4	0.4274094	1.906463
Axon guidance	EPHA3//EPHB3//GNAI3//NFATC1//NGEF//SRGAP2	0.4274094	1.558493
Pantothenate and CoA biosynthesis	ENPP1//PANK1	0.4274094	1.446841
T cell receptor signaling pathway	CBLB//FOS//MALT1//MAP3K8//NFATC1	0.4274094	1.371352
Valine, leucine and isoleucine degradation	ABAT//AUH//HADH	0.04266307	1.369948
Down-regulated			
Osteoclast differentiation	CSF1R//FCGR2A//NCF2//OSCAR//PLCG2	0.02148696	1.667825
Mineral absorption	SLC30A1//SLC8A1//STEAP1	0.02545406	1.594243
Glycosaminoglycan biosynthesis-heparan sulfate	HS3ST2//NDST2	0.04130237	1.384025

Table 4. Partial list of up-regulated genes at the differentiation

Gene name (Homo sapines)	Genebank Accession	Chromosome	Strand	Description
DYNC1I1	NM_001135557	chr7	+	Dynein, cytoplasmic 1, intermediate chain 1
BNC2	NM_017637	chr9	-	Basonuclin 2
ENPP1	NM_006208	chr6	+	Ectonucleotide pyrophosphatase/phosphodiesterase 1
FBXO42	NM_018994	chr1	-	F-box protein 42
JMY	NM_152405	chr5	+	Junction mediating and regulatory protein, p53 cofactor
NFATC1	NM_006162	chr18	+	Nuclear factor of activated T-cells, cytoplasmic, calcineurin-dependent 1
PLCE1	NM_016341	chr10	+	Phospholipase C, epsilon 1
RAB22A	NM_020673	chr20	+	RAB22A, member RAS oncogene family
TCFL5	NM_006602	chr20	-	Transcription factor-like 5 (basic helix-loop-helix)
CDKN2C	NM_001262	chr1	+	Cyclin-dependent kinase inhibitor 2C
KDSR	NM_002035	chr18	-	3-ketodihydrosphingosine reductase
MALT1	NM_173844	chr18	+	Mucosa associated lymphoid tissue lymphoma translocation gene 1
NET1	NM_001047160	chr10	+	Neuroepithelial cell transforming 1

Table 5. Partial list of down-regulated genes at the differentiation

Gene name (Homo sapines)	Genebank Accession	Chromosome	Strand	Description
DNMT3A	NM_022552	chr2	-	DNA-methyltransferase 3 alpha
PLCG2	NM_002661	chr16	+	Phospholipase C, gamma 2 (phosphatidylinositol-specific)
ANXA11	NM_001157	chr10	-	Annexin A11
GRK6	NM_002082	chr5	+	G protein-coupled receptor kinase 6
HSP90B1	NM_003299	chr12	+	Heat shock protein 90 kDa beta, member 1
KEAP1	NM_012289	chr19	-	Kelch-like ECH-associated protein 1
NDST2	NM_003635	chr10	-	N-deacetylase/N-sulfotransferase 2
NSMAF	NM_001144772	chr8	-	Neutral sphingomyelinase activation associated factor
TSPAN14	NM_001128309	chr10	+	Tetraspanin 14
VCP	NM_007126	chr9	-	Valosin-containing protein
DUSP3	NM_004090	chr17	-	Dual specificity phosphatase 3
GTPBP5	NM_015666	chr20	+	GTP binding protein 5
INSIG1	NM_198336	chr7	+	Insulin induced gene 1
OSMR	NM_003999	chr5	+	Oncostatin M receptor
PPP1CA	NM_206873	chr11	-	Protein phosphatase 1, alpha isoform
SLC23A2	NM_005116	chr20	-	Solute carrier family 23, member 2

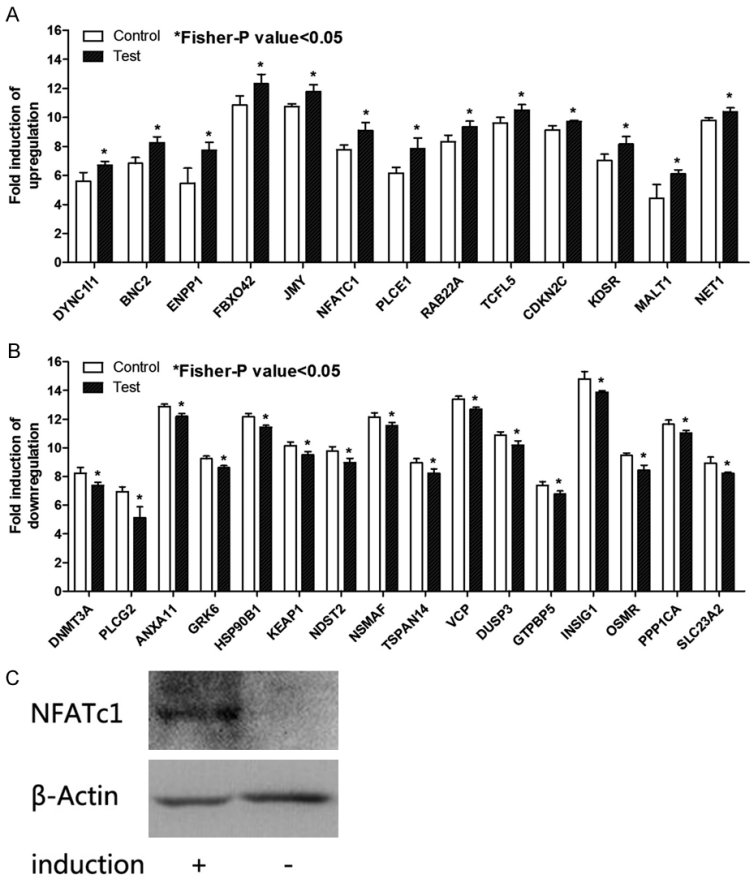

Figure 6. A: 16 down-regulated genes at the differentiation, B: 14 up-regulated genes at the differentiation. C: The expression of NFATc1 was assessed at the protein level by Western blot. Validation of microarray results by real-time PCR. The results represent quantification of mRNA levels relative to β-actin. Normalized expression values obtained by real-time PCR (N = 24).

three-dimensional (3D) environment that allows cell-cell interactions similar to those observed in precartilage condensations found during embryonic development. We had been interested in exploring crucial genes and pathways during the early stage of chondrogenesis. Thus, the 3D pellet model was applied to evaluate the chondrogenic potential of MSCs [11]. In this study, we have demonstrated that the induced pellet tissues were homogenous and similar to the layered structure of human cartilage. Our histological findings showed that hMSCs are able to undergo differentiation into cartilage as Alcian-blue staining was shown surrounding the cartilage matrix, illustrating that cells found in the outer layer had induced fibrocartilage-like features. The chondrogenic marker gene collagen II was highly expressed surrounding the pellet, and hypertrophy, as shown by the large cavities formed by hypertrophic cells, was also found in the internal area. Moreover, these protein changes were consistent with our microarray studies on samples undergoing the early stage of chondrogenesis. Furthermore, the 30 genes identified in the microarray as being differentially expressed were measured via qRT-PCR and similar expression fold changes were observed, which provides additional support for the reliability of our microarray data.

During chondrogenesis, Sox9 is required for mesenchymal cell condensation and the expression of cartilage-specific ECM genes [12]. The marker genes, including collagen IIa1, aggrecan, and collagen Xa1, were all upregulated compared with the control at days 14 and 21. The onset of chondrogenic differentiation was marked by Sox9, its mRNA expression level started increasing at day 14, and reached the maximum level at day 21. Some studies have indicated that mouse embryos at different stages (E18.5 days) [13] are flanked with growth plates in which chondrocytes proceed layer per layer through their successive maturation stages, which was shown with Alcian blue staining (specific for aggrecan in cartilage). This is consistent with our findings in this study.

The identified differential genes were annotated in the GO format for biological function classification and in the pathway analysis format for hMSCs chondrogenesis. Profiling identified a subset of the total number of probes analyzed by Agilent whole-genome oligo microarray. We identified 16 down- and 14 upregulated genes in the process. In the GO analysis, the identified genes, including T cell receptor signaling (P = 7.37E-16) and antigen receptor-mediated signaling (P = 7.52E-05), were overrepresented while the underrepresented processes included skeletal system (P = 7.52E-05) and acute inflammatory response (P = 7.52E-05). Here,

two important pathways associated with the outcome of hMSC differentiation were identified. (1) The upregulation of the T cell receptor signaling pathway. [Ca^{2+}] acts as a switch for NFAT activity by regulating its phosphorylation status. In the cytoplasm of resting cells, dephosphorylated NFAT (mediated by [Ca^{2+}]) translocates to the nucleus and binds to its target promoter regions. In our previous study, we identified a regulator of Sox9 as NFATc1, which directly binds to the promoter of Sox9. These results are evidence that NFATc1 protein could bind to the promoter region of Sox9, initiating transcription and triggering expression of the marker genes. (2) The downregulation of skeletal system development. PLCG2 and SLC30A1 downregulate not only Zn^{2+} influx but also Ca^{2+} influx, thereby protecting cells from the effects of excessive cation permeation [14]. These pathways were both involved in osteoclast differentiation and mineral absorption.

The results are completely from the whole genome microarray data of hMSC pellets at the end of 3 days of chondrogenic differentiation. Our results revealed the expression of several important genes involved in complement and coagulation cascade, complement activity, metabolism and cell differentiation, proliferation, and apoptosis. These data provide a roadmap for future studies. Moreover, we identified that the gene expression of NFATc1 was also upregulated in the differentiation. We believe NFATc1 could also participate in chondrogenesis regulation and may interact with the master transcriptional regulator Sox9. However, a great deal of further study is needed to understand the true biological activities of the *NFATc1* gene and identify other genes involved in differentiation, either by gene addition, protein-protein interaction or other methods.

Acknowledgements

This work was supported by Key program of National Natural Science Foundation of China (No. 31430030); Sanming Project of Medicine in Shenzhen (SZSM201609028); Traditional Chinese Medicine Project of Guangdong Provincial (No. 20152061) and National Natural Science Foundation of China (Grant No. 8160-0606).

Disclosure of conflict of interest

None.

Address correspondence to: Xuenong Zou, Department of Spinal Surgery, The First Affiliated Hospital of Sun Yat-sen University, No. 58, Zhongshan 2nd Road, Guangzhou 510080, P. R. China. Tel: +86-13316831982; Fax: +86-13316831982; E-mail: znxueyy@163.com

References

[1] Neuss S, Denecke B, Gan L, Lin Q, Bovi M, Apel C, Wöltje M, Dhanasingh A, Salber J, Knüchel R and Zenke M. Transcriptome analysis of MSC and MSC-derived osteoblasts on resomer® LT706 and PCL: impact of biomaterial substrate on osteogenic differentiation. PLoS One 2011; 6: e23195.

[2] Schipani E and Clemens TL. Hypoxia and the hypoxia-inducible factors in the skeleton. IBMS BoneKEy 2008; 5: 275-284.

[3] Tomita M, Reinhold MI, Molkentin JD and Naski MC. Calcineurin and NFAT4 induce chondrogenesis. J Biol Chem 2002; 277: 42214-42218.

[4] Gwack Y, Feske S, Srikanth S, Hogan PG and Rao A. Signalling to transcription: store-operated Ca2+ entry and NFAT activation in lymphocytes. Cell Calcium 2007; 42: 145-156.

[5] Macian F. NFAT proteins: key regulators of T-cell development and function. Nat Rev Immunol 2005; 5: 472-484.

[6] Viola JP, Carvalho LD, Fonseca BP and Teixeira LK. NFAT transcription factors: from cell cycle to tumor development. Braz J Med Biol Res 2005; 38: 335-344.

[7] Zanotti S and Canalis E. Notch suppresses nuclear factor of activated T cells (NFAT) transactivation and Nfatc1 expression in chondrocytes. Endocrinology 2013; 154: 762-772.

[8] Lin SS, Tzeng BH, Lee KR, Smith RJ, Campbell KP and Chen CC. Cav3.2 T-type calcium channel is required for the NFAT-dependent Sox9 expression in tracheal cartilage. Proc Natl Acad Sci U S A 2014; 111: E1990-E1998.

[9] Ranger AM, Gerstenfeld LC, Wang J, Kon T, Bae H, Gravallese EM, Glimcher MJ and Glimcher LH. The nuclear factor of activated T cells (NFAT) transcription factor NFATp (NFATc2) is a repressor of chondrogenesis. J Exp Med 2000; 191: 9-22.

[10] Greenblatt MB, Ritter SY, Wright J, Tsang K, Hu D, Glimcher LH and Aliprantis AO. NFATc1 and NFATc2 repress spontaneous osteoarthritis. Proc Natl Acad Sci U S A 2013; 110: 19914-19919.

[11] Pelttari K, Steck E and Richter W. The use of mesenchymal stem cells for chondrogenesis. Injury 2008; 1: S58-S65.

[12] Tew SR, Li Y, Pothacharoen P, Tweats LM, Hawkins RE and Hardingham TE. Retroviral

transduction with SOX9 enhances re-expression of the chondrocyte phenotype in passaged osteoarthritic human articular chondrocytes. Osteoarthritis Cartilage 2005; 13: 80-89.

[13] Lefebvre V and Smits P. Transcriptional control of chondrocyte fate and differentiation. Birth Defects Res C Embryo Today 2005; 75: 200-212.

[14] Segal D, Ohana E, Besser L, Hershfinkel M, Moran A and Sekler I. A role for ZnT-1 in regulating cellular cation influx. Biochem Biophys Res Commun 2004; 323: 1145-1150.